

## Spreading of Perturbations in Long-Range Interacting Classical Lattice Models

David Métivier,<sup>1,2,3</sup> Romain Bachelard,<sup>4</sup> and Michael Kastner<sup>2,3,\*</sup>

<sup>1</sup>*Université de Lyon, École Normale Supérieure de Lyon, 46 Allée d'Italie, 69364 Lyon cedex 07, France*

<sup>2</sup>*National Institute for Theoretical Physics (NITheP), Stellenbosch 7600, South Africa*

<sup>3</sup>*Institute of Theoretical Physics, University of Stellenbosch, Stellenbosch 7600, South Africa*

<sup>4</sup>*Instituto de Física de São Carlos, Universidade de São Paulo, 13560-970 São Carlos, SP, Brazil*

(Received 13 January 2014; revised manuscript received 9 May 2014; published 28 May 2014)

Lieb-Robinson-type bounds are reported for a large class of classical Hamiltonian lattice models. By a suitable rescaling of energy or time, such bounds can be constructed for interactions of arbitrarily long range. The bound quantifies the dependence of the system's dynamics on a perturbation of the initial state. The effect of the perturbation is found to be effectively restricted to the interior of a causal region of logarithmic shape, with only small, algebraically decaying effects in the exterior. A refined bound, sharper than conventional Lieb-Robinson bounds, is required to correctly capture the shape of the causal region, as confirmed by numerical results for classical long-range  $XY$  chains. We discuss the relevance of our findings for the relaxation to equilibrium of long-range interacting lattice models.

DOI: 10.1103/PhysRevLett.112.210601

PACS numbers: 05.50.+q, 05.60.Cd, 45.05.+x

In many nonrelativistic lattice systems, and despite the absence of Lorentz covariance, physical effects are mostly restricted to a causal region, often in the shape of an effective “light cone,” with only tiny effects leaking out to the exterior. The technical tool, known as the Lieb-Robinson bound [1,2], to quantify this statement in a quantum mechanical context is an upper bound on the norm of the commutator  $[O_A(t), O_B(0)]$ , where  $O_A(0)$  and  $O_B(0)$  are operators supported on the subspaces of the Hilbert space corresponding to nonoverlapping regions  $A$  and  $B$  of the lattice. The importance of such a bound lies in the fact that a multitude of physically relevant results can be derived from it. Examples are bounds on the creation of equal-time correlations [3], on the transmission of information [4], and on the growth of entanglement [5], the exponential spatial decay of correlations in the ground state of a gapped system [6], or a Lieb-Schultz-Mattis theorem in higher dimensions [7]. Experimental observations related to Lieb-Robinson bounds have also been reported [8].

The original proof by Lieb and Robinson [1] requires interactions of finite range. An extension to power-law-decaying long-range interactions has been reported in Refs. [3,6]. In this case the effective causal region is no longer cone shaped, and the spatial propagation of physical effects is not limited by a finite group velocity [9]. For “strong long-range interactions,” i.e., when the interaction potential decays proportionally to  $1/r^\alpha$  with an exponent  $\alpha$  smaller than the lattice dimension  $d$ , the theorems in [3,6] do not apply and no Lieb-Robinson-type results are known. This fact nicely fits into the larger picture that, for  $\alpha \leq d$ , the behavior of long-range interacting systems often differs substantially from that of short-range interacting systems. Examples of such differences include nonequivalent equilibrium statistical ensembles and negative

response functions [10], or the occurrence of quasistationary states whose lifetimes diverge with the system size [11,12]. The latter is a dynamical phenomenon, and it has been conjectured in [13] that some of its properties are universal and in some way connected to Lieb-Robinson bounds.

In most cases the peculiarities of long-range interacting systems have been investigated in the framework of classical Hamiltonian systems [12], but little is known about Lieb-Robinson bounds in classical mechanics. Exceptions are restricted to specific models with nearest-neighbor interactions [14,15]. In the context of classical Hamiltonian mechanics, a Lieb-Robinson bound is an upper bound on the norm of the Poisson bracket  $\{f_A(0), g_B(t)\}$ , where  $f_A(0)$  and  $g_B(0)$  are phase space functions supported only on the subspaces of phase space corresponding to the nonoverlapping regions  $A$  and  $B$  of the lattice, respectively. The physical meaning of the norm of this Poisson bracket becomes evident from an expression put forward in [14],

$$|\{f_A(0), g_B(t)\}| \leq |A||B| \|\nabla f\|_\infty \|\nabla g\|_\infty u_{AB}(t), \quad (1)$$

where  $\|\nabla f\|_\infty$  and  $\|\nabla g\|_\infty$  are the (bounded) maxima of all the partial derivatives of  $f$  and  $g$  with respect to the phase space coordinates, and

$$u_{AB}(t) = 4 \max_{\substack{i \in A \\ j \in B}} \left\{ \left| \frac{\partial p_j(t)}{\partial p_i(0)} \right|, \left| \frac{\partial q_j(t)}{\partial p_i(0)} \right|, \left| \frac{\partial p_j(t)}{\partial q_i(0)} \right|, \left| \frac{\partial q_j(t)}{\partial q_i(0)} \right| \right\}. \quad (2)$$

The partial derivatives on the right-hand side of (2) quantify the effect that a variation of the initial momentum or position  $p_i(0)$ ,  $q_i(0)$  at the lattice site  $i$  has on the

time-evolved momentum or position  $p_j(t)$ ,  $q_j(t)$  at the lattice site  $j$ . A classical Lieb-Robinson bound is therefore a measure for the spreading in time and space of an initial perturbation, with potential applications to a broad range of physical processes, including heat conduction, signal transmission, transfer of energy, or the approach to equilibrium.

In this Letter we study the spreading in time and space of initial perturbations in classical long-range interacting lattice models. We have proved a Lieb-Robinson-type result, providing an upper bound on  $u_{AB}(t)$  in (2) [and hence on the Poisson bracket (1)] for a broad class of classical long-range interacting lattice models in arbitrary spatial dimension. Dipolar interactions in condensed matter systems are the prime example of such long-range interacting lattice systems [16], but many other examples exist [17]. To avoid the rather technical notation of the general result [18], we present the main result in this Letter for a specific class of systems, namely classical  $XY$  models in  $d$  spatial dimensions with pair interactions that decay like a power law  $1/|i-j|^\alpha$  with the (1-norm) distance  $|i-j|$  between lattice sites  $i$  and  $j$ . The value of the exponent  $\alpha$  determines the range of the interaction, from mean-field-type (distance-independent) interactions at  $\alpha = 0$  to nearest-neighbor couplings in the limit  $\alpha \rightarrow \infty$ .

Our study focuses on the influence of the interaction range on the spreading of perturbations, and we find pronounced quantitative and qualitative changes upon variation of  $\alpha$ . Different from systems with finite-range interactions, the effect of an initial perturbation is found to be effectively restricted to the interior of a causal region of logarithmic shape, with algebraically small effects in the exterior. Similar to the short-range case, such a bound can be used to rigorously control finite-size effects in simulations of lattice models, exclude information transmission above a certain measurement resolution in the exterior of the effective causal region, and much more. Our analytical results are supplemented by numerical simulations of the time evolution of a long-range interacting  $XY$  chain. Besides confirming the validity of the bound, the numerical results reveal that the refined version of our bound, sharper than conventional Lieb-Robinson-type bounds, is required in order to correctly capture the shape of the propagation front.

*$\alpha XY$  model.*—This model consists of classical  $XY$  spins (or rotors) attached to the sites  $i \in \Lambda$  of a  $d$ -dimensional hypercubic lattice  $\Lambda \subset \mathbb{Z}^d$ . The phase space of a single rotor is  $X_i = \mathbb{S}^1 \times \mathbb{R}$ , allowing us to parametrize each rotor by an angular variable  $q_i \in \mathbb{S}^1$  and by its angular momentum  $p_i \in \mathbb{R}$ . On the phase space  $\mathbb{X} = X_1 \times \cdots \times X_{|\Lambda|}$  of the total system, we define the Hamiltonian function

$$H = \sum_{i \in \Lambda} \frac{p_i^2}{2} - \frac{J_\Lambda}{2} \sum_{\substack{i, j \in \Lambda \\ i \neq j}} \frac{\cos(q_i - q_j)}{|i-j|^\alpha}. \quad (3)$$

For  $\alpha \leq d$ , the second sum on the right-hand side of (3) is superextensive, i.e., asymptotically for large lattices it grows faster than linearly with the number  $|\Lambda|$  of lattice sites. Our proof of a Lieb-Robinson bound requires the Hamiltonian to be extensive. We enforce extensivity also for  $\alpha \leq d$  by allowing the coupling constant to depend explicitly on the lattice,

$$J_\Lambda = J / \sup_{i \in \Lambda} \sum_{j \in \Lambda \setminus \{i\}} \frac{1}{|i-j|^\alpha}, \quad (4)$$

where  $J$  is a real constant [19].

*Classical long-range Lieb-Robinson bound.*—Upper bounds on the partial derivatives on the right-hand side of (2) are given by

$$\left| \frac{\partial q_j(t)}{\partial q_i(0)} \right| \leq \frac{\sum_{n=1}^{\infty} \frac{U_n^{ij} t^{2n}}{(2n)!}}{|i-j|^\alpha} \leq \frac{\cosh(vt) - 1}{|i-j|^\alpha} =: B_{ij}^{qq}(t), \quad (5a)$$

$$\left| \frac{\partial q_j(t)}{\partial p_i(0)} \right| \leq \frac{\sum_{n=1}^{\infty} \frac{U_n^{ij} |t|^{2n+1}}{(2n+1)!}}{|i-j|^\alpha} \leq \frac{\sinh|vt| - |vt|}{v|i-j|^\alpha} =: B_{ij}^{qp}(t), \quad (5b)$$

$$\left| \frac{\partial p_j(t)}{\partial q_i(0)} \right| \leq \frac{\sum_{n=1}^{\infty} \frac{U_n^{ij} |t|^{2n-1}}{(2n-1)!}}{|i-j|^\alpha} \leq \frac{v \sinh|vt|}{|i-j|^\alpha} =: B_{ij}^{pq}(t), \quad (5c)$$

$$\left| \frac{\partial p_j(t)}{\partial p_i(0)} \right| \leq \frac{\sum_{n=1}^{\infty} \frac{U_n^{ij} t^{2n}}{(2n)!}}{|i-j|^\alpha} \leq \frac{\cosh(vt) - 1}{|i-j|^\alpha} =: B_{ij}^{pp}(t). \quad (5d)$$

The positive coefficients  $U_n^{ij}$  are defined recursively by

$$U_{n+1}^{ij} = \begin{cases} |J| U_n^{ij} + |J_\Lambda| U_n^{ii} + C_{ij} U_n^{\max} & \text{for } i \neq j, \\ |J| U_n^{ii} + C_{ii} U_n^{\max} & \text{for } i = j, \end{cases} \quad (6)$$

with  $U_1^{ij} = |J_\Lambda|$  and  $U_1^{ii} = |J|$ , and we use the constants

$$U_n^{\max} = \sup_{i, j \in \Lambda} U_n^{ij}, \quad v = \sup_{i, j \in \Lambda} \sqrt{|J + J_\Lambda| + C_{ij}}, \quad (7)$$

$$C_{ij} = \begin{cases} |J_\Lambda| \sum_{k \in \Lambda \setminus \{i, j\}} \frac{|i-j|^\alpha}{|i-k|^\alpha |j-k|^\alpha} & \text{for } i \neq j, \\ |J_\Lambda| \sum_{k \in \Lambda \setminus \{i\}} \frac{1}{|i-k|^{2\alpha}} & \text{for } i = j. \end{cases} \quad (8)$$

The proof of the bounds combines techniques for classical lattices with nearest-neighbor interactions [14] with those used for proving Lieb-Robinson bounds for long-range quantum systems [3,6], with the additional refinement of allowing lattice-dependent coupling constants. In the thermodynamic limit of infinite lattice size, the quantity  $v$  in (7) remains finite and hence the bounds remain meaningful [18].

All the bounds on the right-hand side of (5a)–(5d), and therefore also the norm of the Poisson bracket (1), grow exponentially for large times  $|t|$ , and decay as a power law with the distance  $|i - j|$ . For some  $\epsilon > 0$ , the effect of a perturbation is therefore smaller than  $\epsilon$  outside a region in the  $(|i - j|, t)$ -plane specified, for large  $|t|$ , by

$$v|t| > \ln(2\epsilon) + \alpha \ln|i - j|. \quad (9)$$

This effective causal region, in which the effect of an initial perturbation is non-negligible, has a logarithmic shape, and differs in this respect from the linear (cone-shaped) region derived in [14] for short-range interactions. As a consequence, no finite group velocity limits the spreading of perturbations in long-range interacting lattices, and supersonic propagation can occur. For a refined understanding of the spatiotemporal behavior, we go beyond the usual Lieb-Robinson-type estimates and consider the sharper bounds in (5a)–(5d), where the coefficients  $U_n^{ij}$  introduce an additional spatial dependence. The functional form of these bounds will be illustrated below, and we also show that only the sharper bounds correctly capture the shape of the propagation front.

The bounds (5a)–(5d) remain valid, with only minor modifications of the parameters and prefactors, under broad generalizations, including arbitrary graphs  $\Lambda$ , multidimensional single-particle phase spaces  $X_i$ , many-particle interactions, and very general forms of the interaction potential [18]. In the remainder of this Letter we subject the bounds (5a)–(5d) to a reality check, in the sense of testing their tightness and whether the form of the propagation front obtained numerically is faithfully reproduced.

*Numerics.*—We consider the  $\alpha XY$  model (3) on a ring, i.e., a one-dimensional chain of  $N = |\Lambda|$  sites with periodic boundary conditions. The partial derivatives in (5a)–(5d) are approximated by difference quotients,

$$\frac{\partial p_j(t)}{\partial q_i(0)} \approx \frac{\tilde{p}_j(t) - p_j(t)}{\delta q_i} =: Q_{ij}^{pq}(t), \quad (10)$$

and similarly for the other derivatives. Here,  $p_j(t) = p_j(t, p_1(0), \dots, p_N(0), q_1(0), \dots, q_N(0))$  is the time-evolved momentum obtained by starting from a certain initial condition, and  $\tilde{p}_j(t) = p_j(t, p_1(0), \dots, p_N(0), q_1(0), \dots, q_i(0) + \delta q_i, \dots, q_N(0))$  is for a similar initial condition, but with the  $i$ th initial position shifted by some small  $\delta q_i$ . The time-evolved momenta  $p_j$  and  $\tilde{p}_j$  are obtained by numerically integrating Hamilton's equations using a sixth-order symplectic integrator [20]. The numerical results for  $Q_{ij}^{pq}$  fluctuate strongly in time, obscuring the overall trend of the spreading. To reduce the fluctuating background, we compute the difference quotient (10) for 20 different (pairs of) initial conditions; details regarding the choice of initial conditions are given in the Supplemental Material [18]. Since our aim is to compare the numerical

results to the upper bounds (5a)–(5d), we select, for any fixed time  $t$  and lattice sites  $i$  and  $j$ , the largest of the 20  $Q_{ij}^{pq}$ -values. The resulting maximum is denoted by  $\mathcal{Q}_{ij}^{pq}$ , and its time- and distance-dependence is shown in Fig. 1. The plots illustrate the supersonic propagation of perturbations in the presence of long-range interactions, as expected from the inequality (9).

For all distances  $|i - j|$  and times  $t$ , the numerical results are smaller than the bounds (5a)–(5d) and hence confirm their validity. What is more, the results nicely agree with the functional forms of the bounds, and only the prefactors are overestimated. This observation suggests fitting the function  $cB_{ij}^{pq}(t/z)$  to the numerical data of  $\mathcal{Q}_{ij}^{pq}(t)$  (and similarly for the other derivatives), with  $c$  and  $z$  as fit parameters (see left and center plots of Fig. 2). Although the quality of this fit (having a residual sum of squares of 0.157) is acceptable, it can be improved by about two orders of magnitude by using the fit function

$$\tilde{B}_{ij}^{pq}(t) = \frac{\tilde{c}}{|i - j|^\alpha} \sum_{n=1}^{\infty} \frac{U_n^{ij} |t/\tilde{z}|^{2n-1}}{(2n-1)!}, \quad (11)$$

based on the sharper bound in (5c), with fit parameters  $\tilde{c}$  and  $\tilde{z}$ . This fit is of excellent quality, indicating that the distance-dependence of the coefficients  $U_n^{ij}$  in (7) appreciably modifies the shape of the propagation front and correctly reproduces the actual spreading.

The sharper bounds in (5a)–(5d) inherit a system-size dependence through the lattice dependence of  $J_\Lambda$  and  $C_{ij}$  in the coefficients  $U_n^{ij}$ . As a result,  $U_n^{ij}$  (at fixed  $n$  and fixed distance  $|i - j|$ ) scales differently with  $N$  for the cases  $0 \leq \alpha < d/2$ ,  $d/2 < \alpha < d$ , and  $\alpha > d$ , respectively [18]. The switching from one regime to another at  $\alpha = d/2$  and  $\alpha = d$  nicely coincides with the different scaling regimes of equilibration times observed in [13]. Additionally to the  $N$ -dependence inherent to the bound, we find that, for  $\alpha \leq d$ , the optimal values for the fit parameters  $\tilde{c}$  and  $\tilde{z}$  in (11)

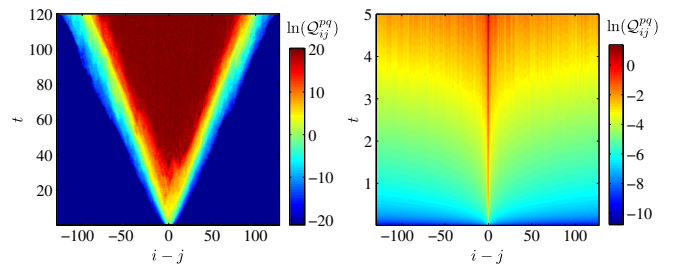


FIG. 1 (color online). Illustration of the spatiotemporal behavior of perturbations. The contour plots show  $\ln \mathcal{Q}_{ij}^{pq}$  as a function of the distance  $|i - j|$  and time  $t$ , for chains of length  $N = 256$ . Left: for the  $XY$  chain with nearest-neighbor interactions, the effect of a perturbation is restricted to the interior of a cone-shaped region. Right: for the  $\alpha XY$  chain with  $\alpha = 1/2$ , the contours spread faster than linearly in space, as expected from (9), illustrating supersonic propagation.

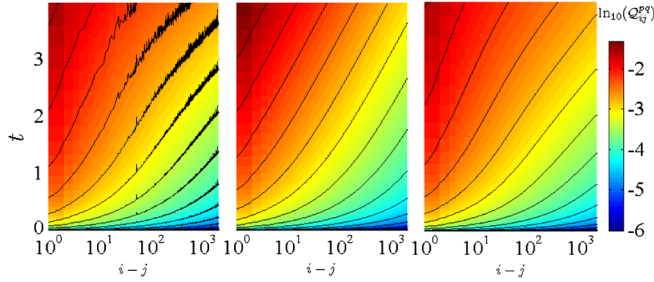


FIG. 2 (color online). Numerical data and fits of the spreading of perturbations in the  $\alpha XY$  chain with  $\alpha = 1/2$ . The contour plots show  $\ln Q_{ij}^{pq}$  as a function of the distance  $|i-j|$  on a logarithmic scale and time  $t$  on a linear scale. Left: numerical data for a chain of length  $N = 4096$ . Center: fit of the function  $cB_{ij}^{pq}(t/z)$  [based on the weaker bound in (5c)] to the numerical data of  $Q_{ij}^{pq}(t)$ , with fit parameters  $c = 0.0064$  and  $z = 1.47$ , yielding a residual sum of squares of 0.157. The contours of the bound are approximately linear for large  $|i-j|$  and  $t$ , but this does not correctly capture the actual behavior of the data. Right: As in the center plot, but fitting the parameters  $\tilde{c} = 21.5$  and  $\tilde{z} = 11.2$  in the stronger bound (11) and yielding a residual sum of squares as small as 0.0065.

show a strong  $N$ -dependence, well-captured by a power law  $\propto N^{(1-\alpha)/2}$  for both parameters (Fig. 3 left and center). This scaling seems to originate from the  $N$ -dependence of the prefactor  $J_\Lambda$  in (3) and (8), and is seen as an indication that the bounds could be further improved. For  $\alpha > d$ , in contrast, the  $N$ -dependence of  $\tilde{c}$  and  $\tilde{z}$  is negligible.

*Comparison to the quantum mechanical bound.*— Lieb-Robinson bounds were previously known for long-range interacting *quantum* systems [3,6]. The functional form of these bounds is  $c(e^{v|t|} - 1)/(1 + |i-j|)^\alpha$ , with a constant  $c$  that depends on the observables considered. Asymptotically for long times  $t$  and large distances  $|i-j|$ , this functional form coincides with that of the weaker form of all four classical bounds (5a)–(5d). For small  $t$ , however, the bounds differ, not only between the classical and the quantum case, but also between the four derivatives bounded in the classical case. The short-time behavior is linear in  $t$  for  $B_{ij}^{pq}$  in (5c), quadratic in  $t$  for  $B_{ij}^{qq}$  and  $B_{ij}^{pp}$  in (5a) and (5d), and cubic in  $t$  for  $B_{ij}^{qp}$  in (5b). The numerical results in Fig. 3 (right) confirm that the real short-time dynamics of the  $\alpha XY$  model is correctly captured by these different functional forms of the bounds. The quantum mechanical bound, in contrast, increases linearly for short times  $t$ , independently of the observables considered, although this may not reflect the actual behavior of expectation values in all cases.

*Conclusions.*— We have reported Lieb-Robinson-type inequalities, bounding the speed at which a perturbation can travel across the lattice, for a broad class of long-range interacting classical lattice models (including models on arbitrary graphs  $\Lambda$ , with multidimensional single-particle phase spaces  $X_i$ , many-particle interactions, and for rather

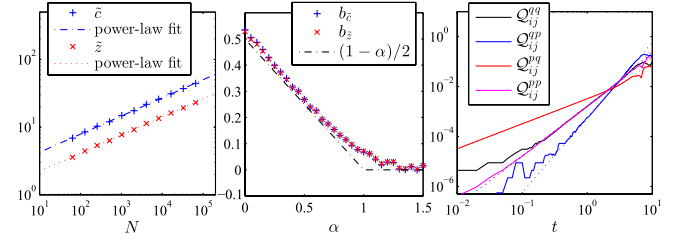


FIG. 3 (color online). Left and center: system-size dependence of the parameters  $\tilde{c}$  and  $\tilde{z}$  when fitting (11) to the numerical data of  $\alpha XY$  chains, using initial conditions with zero initial momenta. The data for  $\alpha = 1/2$  in the left plot are well described by the power laws  $\tilde{c} \approx 2.3N^{b_{\tilde{c}}}$  and  $\tilde{z} \approx 1.2N^{b_{\tilde{z}}}$  with  $b_{\tilde{c}} \approx b_{\tilde{z}} \approx 0.27$ . Right:  $b_{\tilde{c}}$  and  $b_{\tilde{z}}$  as functions of the exponent  $\alpha$ . For  $\alpha < 1$  both are well fitted by the linear function  $(1-\alpha)/2$ . Right: short-time behavior of the difference quotients  $Q_{ij}^{qq}$ ,  $Q_{ij}^{qp}$ ,  $Q_{ij}^{pq}$ , and  $Q_{ij}^{pp}$ , plotted on a log-log scale. Data are for  $\alpha = 1/2$  and chain length  $N = 4096$ . The solid data curves display a linear, quadratic, or cubic initial growth, in agreement with the corresponding bounds. Dotted lines are fits of  $cB_{ij}(t/z)$ , with  $c$  and  $z$  as fitting parameters.

general forms of the interaction potential). By a suitable rescaling, we extended the bounds to arbitrary non-negative long-range exponents  $\alpha$ , deep into the regime of strong long-range interactions. The weaker bounds on the right-hand side of (5a)–(5d) are direct analogs of the quantum mechanical version of Lieb-Robinson bounds for long-range interacting systems [3,6]. While our numerical results for  $\alpha XY$  chains confirm the validity of these bounds, they reveal that the shape of the propagation front is not correctly captured. Only the stronger versions of the bounds in (5a)–(5d), with an additional distance-dependence introduced through the coefficients  $U_n^{ij}$ , reproduce the functional form of the propagation front. These findings are in contrast to the short-range case, where already the weaker “conventional” form of the Lieb-Robinson bound yields the correct, cone-shaped spatiotemporal behavior in agreement with the numerical results.

Since our results apply to arbitrary classical observables, potential applications cover a broad range of dynamical phenomena in long-range interacting classical lattice models, from heat conduction to information transmission, energy transfer, and the approach to equilibrium. In the latter context, different finite-size scaling properties of equilibration times had been observed in the regimes  $0 \leq \alpha < d/2$ ,  $d/2 < \alpha < d$ , and  $\alpha > d$ , respectively [13]. These three regimes agree precisely with the different scaling regimes of the coefficients  $C_{ij}$  that enter and reflect in the bounds (5a)–(5d), providing a theoretical explanation of the numerical observations.

Sharper Lieb-Robinson bounds, similar in spirit to (5a)–(5d), can also be derived for quantum mechanical lattice models with long-range interactions and will be reported in a forthcoming paper.

R. B. acknowledges support by the Fundação de Amparo à Pesquisa do Estado de São Paulo (FAPESP) and the computational support of the Núcleo de Apoio à Óptica e Fotônica (NAPOF-USP). M. K. acknowledges financial support by the National Research Foundation of South Africa via the Incentive Funding and the Competitive Programme for Rated Researchers.

---

\*kastner@sun.ac.za

- [1] E. H. Lieb and D. W. Robinson, *Commun. Math. Phys.* **28**, 251 (1972).
- [2] B. Nachtergaele and R. Sims, in *Entropy and the Quantum, Contemporary Mathematics*, Vol. 529, edited by R. Sims and D. Ueltschi (American Mathematical Society, Providence, 2010); M. Kliesch, C. Gogolin, and J. Eisert, arXiv:1306.0716.
- [3] B. Nachtergaele, Y. Ogata, and R. Sims, *J. Stat. Phys.* **124**, 1 (2006).
- [4] S. Bravyi, M. B. Hastings, and F. Verstraete, *Phys. Rev. Lett.* **97**, 050401 (2006).
- [5] J. Eisert and T. J. Osborne, *Phys. Rev. Lett.* **97**, 150404 (2006).
- [6] M. B. Hastings and T. Koma, *Commun. Math. Phys.* **265**, 781 (2006).
- [7] M. B. Hastings, *Phys. Rev. B* **69**, 104431 (2004).
- [8] M. Cheneau, P. Barmettler, D. Poletti, M. Endres, P. Schauß, T. Fukuhara, C. Gross, I. Bloch, C. Kollath, and S. Kuhr, *Nature (London)* **481**, 484 (2012); T. Langen, R. Geiger, M. Kuhnert, B. Rauer, and J. Schmiedmayer, *Nat. Phys.* **9**, 640 (2013).
- [9] J. Eisert, M. van den Worm, S. R. Manmana, and M. Kastner, *Phys. Rev. Lett.* **111**, 260401 (2013).
- [10] D. Lynden-Bell and R. Wood, *Mon. Not. R. Astron. Soc.* **138**, 495 (1968); W. Thirring, *Z. Phys.* **235**, 339 (1970); R. S. Ellis, K. Haven, and B. Turkington, *J. Stat. Phys.* **101**, 999 (2000); H. Touchette, R. S. Ellis, and B. Turkington, *Physica A (Amsterdam)* **340**, 138 (2004); M. Kastner, *Phys. Rev. Lett.* **104**, 240403 (2010); *J. Stat. Mech.* (2010) P07006.
- [11] M. Antoni and S. Ruffo, *Phys. Rev. E* **52**, 2361 (1995); M. Kastner, *Phys. Rev. Lett.* **106**, 130601 (2011); *Central Eur. J. Phys.* **10**, 637 (2012).
- [12] A. Campa, T. Dauxois, and S. Ruffo, *Phys. Rep.* **480**, 57 (2009).
- [13] R. Bachelard and M. Kastner, *Phys. Rev. Lett.* **110**, 170603 (2013).
- [14] C. Marchioro, A. Pellegrinotti, M. Pulvirenti, and L. Triolo, *J. Stat. Phys.* **19**, 499 (1978).
- [15] P. Buttà, E. Caglioti, S. Di Ruzza, and C. Marchioro, *J. Stat. Phys.* **127**, 313 (2007); H. Raz and R. Sims, *J. Stat. Phys.* **137**, 79 (2009).
- [16] G. Miloshevich, T. Dauxois, R. Khomeriki, and S. Ruffo, *Europhys. Lett.* **104**, 17011 (2013).
- [17] R. Bachelard, T. Manos, P. de Buyl, F. Staniscia, F. S. Cataliotti, G. D. Ninno, D. Fanelli, and N. Piovella, *J. Stat. Mech.* (2010) P06009.
- [18] See Supplemental Material at <http://link.aps.org/supplemental/10.1103/PhysRevLett.112.210601>, which includes Ref. [21].
- [19] Introducing such a normalization is actually a harmless procedure and amounts to a rescaling of time. For a “physical” Hamiltonian without such a rescaling, the bounds we derived hold therefore in rescaled time  $tJ_\Lambda$ . For finite systems, no rescaling is necessary.
- [20] R. I. McLachlan and P. Atela, *Nonlinearity* **5**, 541 (1992).
- [21] P. Hauke and L. Tagliacozzo, *Phys. Rev. Lett.* **111**, 207202 (2013).